

# Examining Human Walking Characteristics with a Telescopic Compass-like Biped Walker Model \*

Seiichi Miyakoshi  
Digital Human Research Center  
National Institute of  
Advanced Industrial Science and  
Technology  
Koto-ku, Tokyo, 135-0064, Japan  
s.miyakoshi@aist.go.jp

Gordon Cheng  
Department of Humanoid Robotics and  
Computational Neuroscience  
ATR Computational Neuroscience Laboratories  
JST-ICORP, Computational Brain Project  
Keihanna, Kyoto, 619-0288, Japan  
gordon@atr.jp

**Abstract** – *A model for biped walking is proposed. The model has a compass-like mechanism with telescopic type legs, and uses a simple leg stretch-contraction motion pattern. The model with a point shaped foot is able to represent human walking characteristics. A systematic conversion from the point shaped foot to the equivalent of a normal surface foot - resembling the shape that of humans, this extension preserves the same human-like walking characteristics while gaining the benefits of added stability and the reduction of impact forces during foot contact.*

**Keywords:** Foot sole profile, motion based shape design, compass-like biped model, partial passive system.

## 1 Introduction

Considerable biped locomotion research has been conducted to date, with much emphasis within the context of humanoid robotics research. These research does not only have direct usages in personal or entertainment or industrial purposes, humanoid robotics (or simulation) research also has the potential of gaining an understanding of the internal mechanism of human - thus a synthetic approach [1]. Consequently, possessing human-like characteristics is especially important for humanoid robots. This paper proposes a motion based human-like foot profile forming. To date, very few studies have treated the topic of the sole shape, and its potential importance, related to walking style and stability.

The zero moment point (ZMP) based control theories [2] have been studied and implemented in biped walking robot [3]. In recent years, humanoids developed by companies, utilizing ZMP-based walking have gained considerable attention [4], [5]. ZMP based control guarantees stability by geometrically keeping ZMP within the convex hull of the contacting surface between foot sole and the ground. Therefore, to maximise the stability, some used box shaped flat foot sole, or just chamfering at the heel and toe. With one noticeable exception, the humanoid robot H7 has a separated

and actuated toe joint like humans, but the reason for the decided structure design parameters was not described [6].

Alternatively, various biped walking approaches are emerged [7], [8], [9], [10], [11], [12] represented by passive dynamic walking [13] and hopping robot [14]. In these approaches, they pay special attention to the intrinsic characteristics of the physical system, and use it to design the mechanics and controllers (sometimes it's implicit). The walking motions derived and implemented experimentally, providing the impression of sophisticated human-like or animal-like behaviours. In these systems, they used point foot, or circular arc profile foot allowing theoretical simplification.

We begin our examination with a point shaped foot model, this model is then extended to an equivalent surface type sole, with subsequent motion pattern, while preserving human-like characteristics - as in the simple point foot model.

In our modelling of human bipedal walking, we attempt to construct the mechanism and motion so that it is also meaningful in the engineering sense. We adopt the assumption that human walking is a very sophisticated and optimum mechanism and motion patterns. Therefore, engineering (efficiency oriented) implementations that utilize the physical characteristics of the system will help in deriving human-like walking.

## 2 Point Foot Model

### 2.1 Partial Passive Mechanism

The model adopted in this paper is a compass-like biped model, which encapsulate human whole body structure into an extremely simple form (see Fig. 1 left). A similar compass-like model has also been studied by [15], [16].

The mechanism of our model is constructed from two bar legs, the upper body is a point mass, point shaped feet, a non-frictional hip joint, and prismatic joints with variable length constraints at the knees. The ground is flat and the contact forces are generated via elastic and viscous-elastic elements in the vertical direction, and via friction elements in the hor-

horizontal direction. A sketch of our model is shown in Fig. 1 center figure.  $\theta$  is the hip joint angle along the vertical axis, a independent value that determines the walking motion pattern. The model is two dimensional, and restricted in the sagittal plane was used in our previous studies [17].

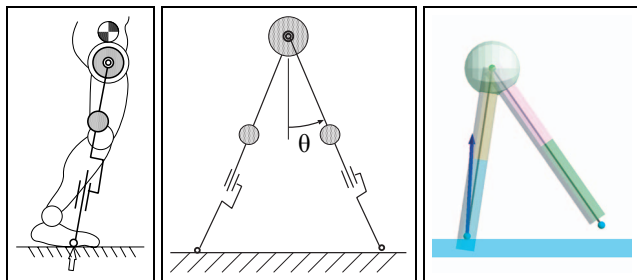


Figure 1: Compass-like biped walker

The mass distribution of the model resembles that of a human [18]. The physical properties of this model is shown in Table 1.

Table 1: Physical parameters of the biped

torso mass	28.3 (kg)
leg mass	7.85 (kg)
leg moment of inertia	0.659 (kg·m <sup>2</sup> )
leg length (neutral position)	1.0 (m)
restitution coefficient	0.0
floor young's modulus	1/10000 of iron's

The dynamical simulator DADS<sup>1</sup> was used to construct the physical model of our system. Our biped model in DADS is shown in Fig. 1 right. The prismatic joints between the legs and the point shaped feet is located near to the center of the legs, and the contact forces are being detected at the point feet.

## 2.2 Simplest Motion Pattern

Changing the length of the legs synchronously with the legs swing generates walking-like motion. The hip joint is not actuated - no controller is included.

The conditions of motion is shown in Fig. 2. Effectively, the simplest walking motion can be generated by stretch and contraction of the legs at 3 times higher the frequency than legs swing.

The initial condition of walking, is by pausing at the exact mid stance phase (the center of Fig. 2 right) and provide a suitable horizontal velocity to the upper-body and the foot of the swinging leg. This form of bipedal walking is considered, as being on the line of the instable equilibrium, so the stability is sensitive to the initial condition.

<sup>1</sup>A commercial product of LMS International.

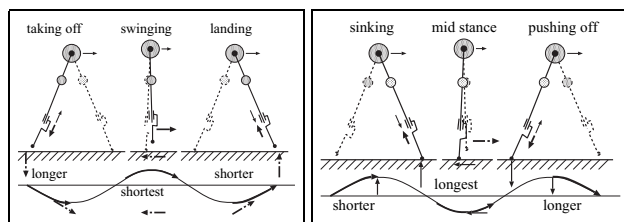


Figure 2: Conditions of swing leg, and extrapolated stance leg

Fine-tuning of the parameters (the amplitude and frequency of sinusoidal stretch and contraction motion, and initial velocity) is required to achieve continuous walking.

## 2.3 Resemblance to Human Walking

Fig. 3 shows the floor reaction force profile for ( $\theta = 0.3(\text{rad})$ ) (see Fig. 1). This plot corresponds to reaction force of humans walking [19]. The solid line represents the right foot, and the dotted line represents the left foot. Both have been normalized by the whole body mass. Correlations of the patterns, magnitudes, and periods can be seen.

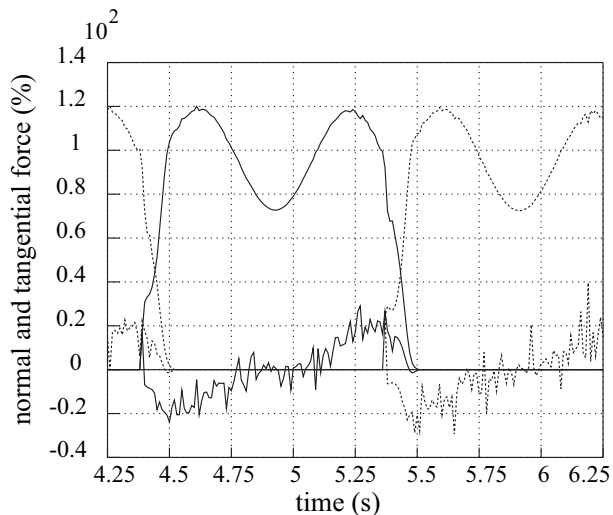


Figure 3: Floor reaction force of the point foot model

The duty factor of double and single support phase can be estimated to be about 20% for one stride. This percentage also correlates to that of humans [20].

A typical floor reaction force plot of ZMP based control can be found in [21]. The measured ground reaction force of the humanoid robot is trapezoid, this is because the controller ensure that the vertical component of the desired trajectory of whole body center of mass being kept constant.

For the sake of comparison, a corresponding reaction force diagram of a passive dynamic walker is shown in Fig.4 left. In contrast to our model, the passive model in Fig. 4 has the same body parameters as our current biped model except for that this model has a surface contact foot, which is mass-less

and hemispheric shaped instead of a point foot. Additionally, the length of the legs is fixed. In order to allow foot clearance of the swing leg, the contact surfaces on the ground exist only around the anticipated foot contact point for a moderate step length akin to steppingstones. The resulting floor reaction force of the passive dynamic walker is flat and the magnitude of the force is almost the same as its body mass.

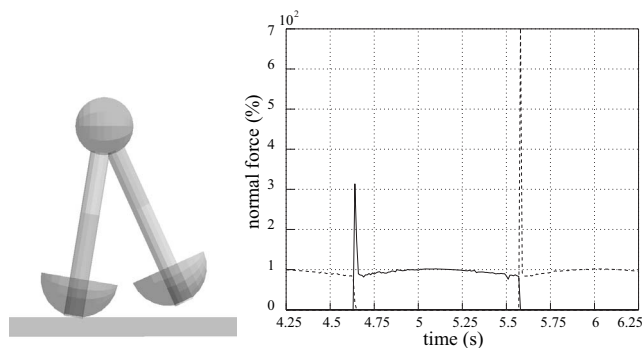


Figure 4: Floor reaction force of the passive dynamic walker

### 3 From point foot to curve sole

Even the extremely simple model (mechanism and motion pattern) in Section 2 can generate human-like bipedal walking motion. We improve this model by introducing a surface sole to the foot.

#### 3.1 Relating Leg Prismatic Motion to Ankle Rotation

In order to obtain the profile of extended sole of the foot, the corresponding extended motion pattern had to be defined. One hypothesis we have taken is that the profile of the sole is optimized for take-off (push-off) and landing. Based on this hypothesis, we divide the foot into two parts: a toe part (take-off) and a heel part (landing), the boundary point is located at the ankle joint. Both the front (toe) part and the back (heel) part can move independently.

The stretch and contraction motion on the prismatic legs represents the sum of whole leg motion (see Fig. 1 left). We introduce additional rotating ankle joint for each leg, then the whole leg stretch and contraction motion is decomposed into two motions, such as, the leg prismatic motion, now which is corresponding to knee bending, and ankle rotating motion (see Fig. 5 left).

The periods of the sinusoidal ankle rotation for each part of the foot are the same as the former prismatic leg motion, but out of phase. This is because these different motions, for the toe at push-off by prismatic leg stretch, and for the heel at landing by prismatic leg contraction, are basically also contributing to the plantar flexion on rotating ankle.

The extended mechanism and motion pattern is shown in Fig. 5. For landing, the prismatic joint of the leg contracts from neutral (the center of the full stroke of the whole leg)

to minimal, while the ankle joint rotates from maximal dorsiflexion to plantar flexion (See Fig. 5 middle and upper half of Fig. 6). On the contrary, for take-off (push-off), the prismatic joint of the leg is fixed at the minimal length, while the ankle joint rotates from dorsiflexion to plantar flexion. (See Fig. 5 right and lower half of Fig. 6). We defined this motion pattern based on the time profile of the power generated at the knee and ankle joints of humans [22]. At the start of the stance phase, the knee joint flexes and the ankle joint moves to plantar flexion to absorb the landing shock/impact. At the end of the stance phase, push-off motion is mainly done by ankle joint plantar flexion.

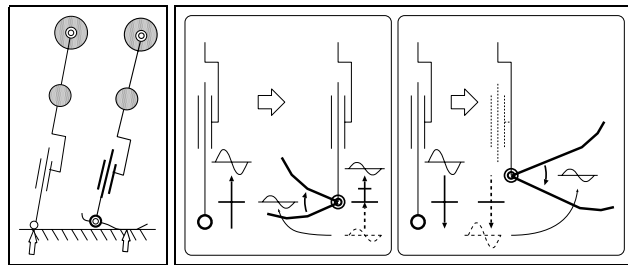


Figure 5: Decompose the leg motion to prismatic knee and rotational ankle motion to transform from point foot to surface foot

The amplitude of the rotating motion at the ankle is defined to be geometrically same as the base angle of the isosceles triangle between the two legs (at its neutral length) and the step length during the double support phase.

#### 3.2 Profiling Foot Sole by Optimizing Aligning Contact Points

Fig. 6 shows a zoomed up sequence of snapshots of the lower leg and foot. In Fig. 6, the sequence is progressing from left to right, and from upper to lower. The direction of walking is from left to right. The left half of the foot is the heel and the right half is the toe. The black filled circle is the mark of the point foot of the former model.

The foot profile is constructed by aligning contacting point elements. The centers of each contacting elements are arranged at a distance 10 (mm) apart. The radius of each contact element is 10 (mm). The vertical displacement of the center of these contact elements in the toe and heel part have been adjusted and optimized for acquiring the most stable walk. The maximum number of regular steps taken, which is the same as the point foot's step length, is used as the criterion function for optimization. At first, we placed additional numbers of contact elements, however after optimization we remove those elements that do not make contact with the floor during walking. We also shorten the sole by eliminating the elements that are placed in a straight line with the terminals of the sole.

Contact points alignment to form the initial foot profile is done manually via a geometric method. The procedure is as follows:

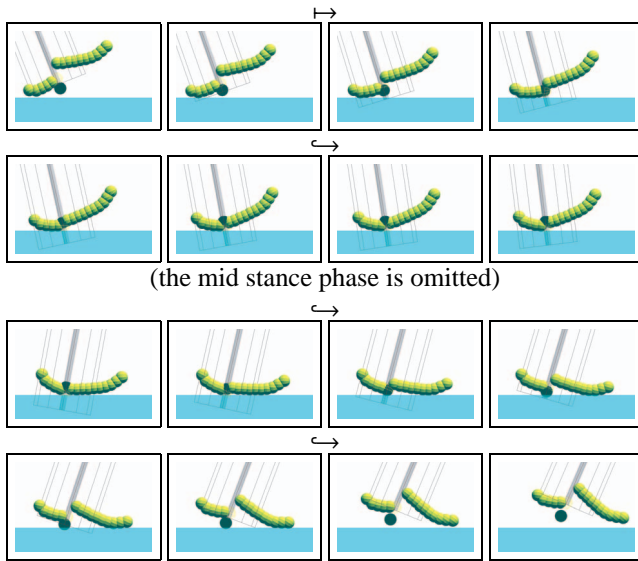


Figure 6: Snap shots of walking by divided foot

1. starting with the former point foot model;
2. aligns the candidates of the contact point elements on the toe and heel (calculation of the contact force of the additional candidate elements are disabled),
3. disable the calculation of the contact force of the point foot, and enable calculation of the contact forces of the newly added contact points.

### 3.3 Sole Profile

Fig. 7 is the acquired sole profile after optimization. The right is the toe, and the left is the heel. The wireframe column drawn is the lower leg. The shape, the scale and the proportion resemble that of a human foot. The slope angle at the toe appears steeper than humans. It is considered that an equivalent structure appears to compensate for the flexion of the foot thumb on a rigid sole.

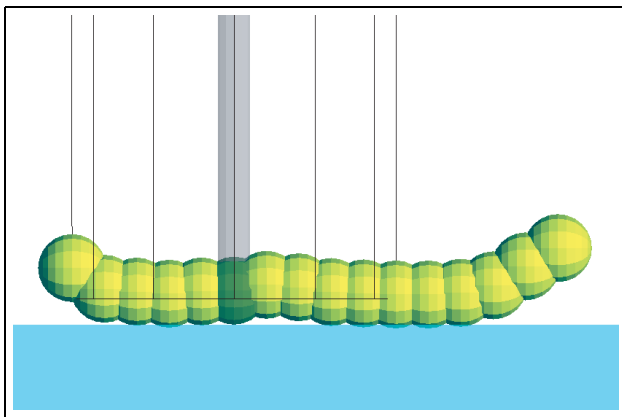


Figure 7: Foot shape

The same optimization process to acquire a sole profile can be done without using 3 times higher frequency than leg swing at the ankle. Fig. 8 shows an example of the shape of the foot sole with the same (exact) frequency as the leg swing. The resulting shape becomes much longer than the human foot size. This could possibly suggest a tradeoff between static stability and generation of effective motion.

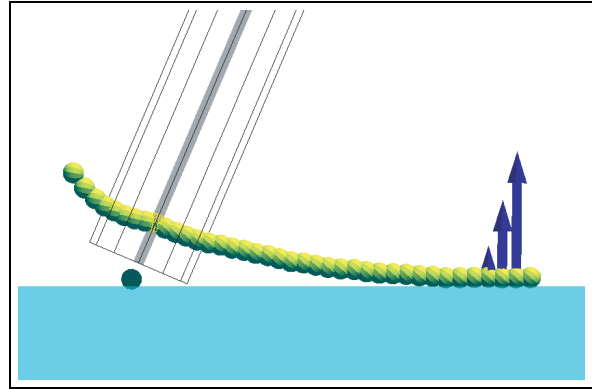


Figure 8: Different foot shape with lower frequency at the ankle

### 3.4 Motion on Unified Sole

In the previous section, we use a divided sole to simplify our studies, but actual humans sole is not divided. To change the sole to a unified one, motion pattern at the ankle is required. We expect that by introducing flexible elements at the ankle joint will ease impact on landing. This is due to the fact that without flexible elements greater impact during touch down will occur (see Fig. 4), producing undesirable perturbation that will effect stability. For instance, touch down impact at the start of the double support phase, perturbing the launching velocity of the upper body. This impact perturbation also affects the end of the double support phase (the push-off phase).

We designed the ankle rotating motion pattern based on reusing the actuation scheme for the divided foot (see Fig. 9). These two rotational actuators are out of phase, as described. We put rotational flexible elements at the ankle joint between each actuators and the foot body. One foot is actuated in antagonistic manner via the two flexible elements. By periodically scheduling the elastic and viscous-elastic parameters of the flexible elements, the sole moves with the heel actuator dominating at the landing phase, and with the toe actuator dominating at the push-off phase. The periodically scheduling is implemented via a PD (proportional-derivative) controller in scheduling its PD gains (Fig. 12).

To acquire continuous walking, optimization of the PD gain parameters for each walking phases is needed, under similar condition with fixed shape foot sole.

The acquired walking motion pattern is shown in Fig. 10. Owing to symmetric motion, the right leg is omitted to simplify presentation. The general appearance of the motion re-

sembles human walking. Fig. 11 provides a plot of the floor reaction force of the new model walking. The solid line is for the right foot, and the dashed line is for the left foot, with low pass filtered, and dotted lines is the raw plot. The two peaks profile is preserved, while noise increases, because of PD gains switching for the flexible elements, each walking phase is in tune with the scheduled gains changes.

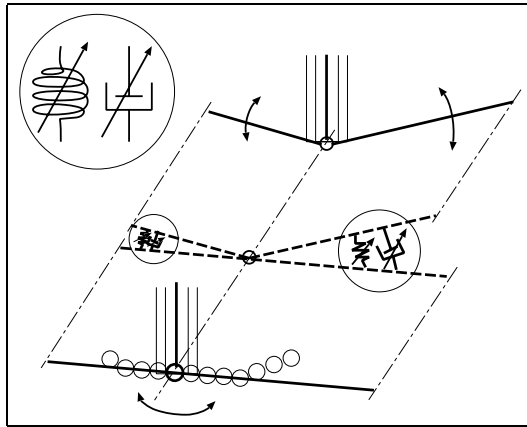


Figure 9: Schema to Combine a toe and heel motion to a sole motion via compliant elements scheduled by walking phase in antagonistic actuation

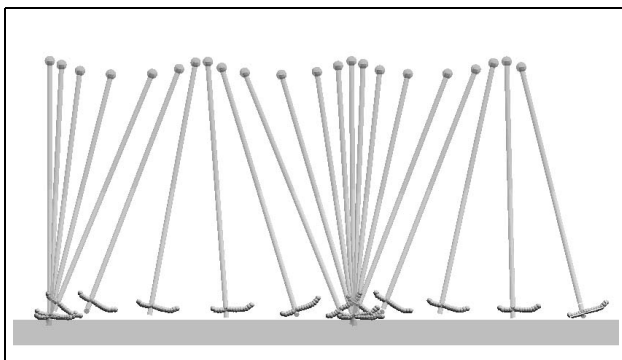


Figure 10: Walking with unified sole (left foot)

Fig. 12 shows the optimized gain parameters of each ankle joint. In the Fig. 12, the solid line and dashed line show the proportional and derivative gains of the right ankle joint. Due to symmetry, we use the same PD gain parameters for both joints. The positive value shows when the toe controller is dominant, and the negative value shows when the heel controller is dominant, these lines shows the totaled value of the toe and heel PD gains. Increasing and decreasing of the damping (derivative) parameter corresponds to the spring (proportional) parameter on the same side. The gains of right ankle joint increase at the moment of push-off (at 1.5s). On the contrary, at landing (at 0.5s), the magnitude of the negative value (activity of the controller) is small. The low PD gains at the landing phase show the passive (loose servoing)

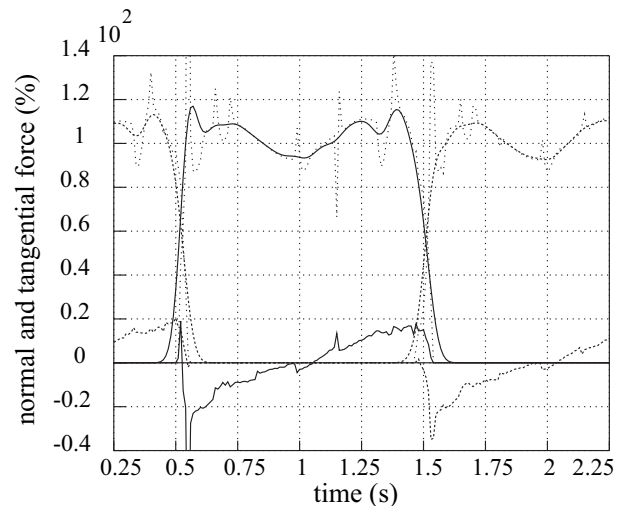


Figure 11: Floor reaction force of the unified sole model

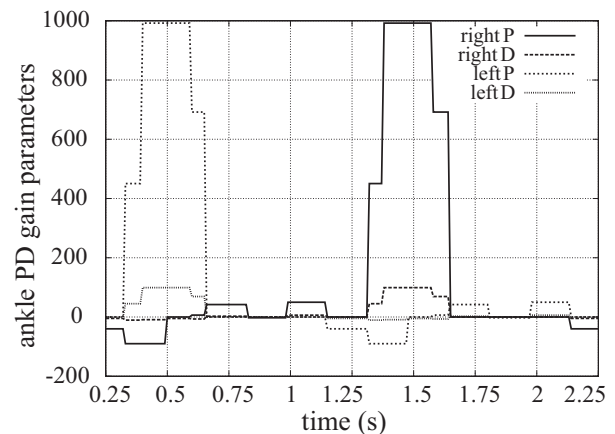


Figure 12: Gain scheduling of the ankle PD parameters as spring and damper coefficients

motion compared with tight tracking of the desired trajectory at the push-off phase caused by the high PD gains.

## 4 Conclusion

We proposed a method to acquire a surface foot profile, extended from a point foot model. This extended foot profile resembles the humans foot profile, and possesses similar characteristics to human walking. Despite of its simplicity our model was also represents characteristics of human walking motion.

## 5 Future Work

Extension to three dimensions is important step in our future works. We contemplate that the biggest problem for this extension would be the handling of perturbations, due to twisting motion, and additional freedom in the frontal plane.

To suppress the occurrence of the twisting torque, we anticipate a push-off based walking model is better suited than a hip joint actuated leg model, especially for high speed walking.

## Acknowledgement

This research was financially supported by COE, and is supported by CREST JST.

We are very grateful to Yasuo Kuniyoshi and Gentaro Taga for helpful suggestions and observations.

## References

- [1] Y. Kuniyoshi and A. Nagakubo, "Humanoid As a Research Vehicle Into Flexible Complex Interaction", Proc. of IROS, Vol. 2, pp. 811–820, 1997.
- [2] M. Vukobratović, B. Borovac, D. Surla and D. Stokić, *Biped Locomotion*, Springer-Verlag, 1990.
- [3] A. Takanishi, T. Takeya, H. Karaki and I. Kato, "A Control Method for Dynamic Biped Walking Under Unknown External Force", Proc. of IROS, Vol. 2, pp. 795–801, 1990.
- [4] K. Hirai, M. Hirose, Y. Haikawa and T. Takenaka, "The Development of Honda Humanoid Robot", Proc. of ICRA, Vol. 2, pp. 1321–1326, 1998.
- [5] Y. Kuroki, M. Fujita, T. Ishida, K. Nagasaka and J. Yamaguchi, "A small biped entertainment robot exploring attractive applications", Proc. of ICRA, Vol. 1, pp. 471–476, 2003.
- [6] K. Nishiwaki, S. Kagami, Y. Kuniyoshi, M. Inaba and H. Inoue, "Toe Joints that Enhance Bipedal and Full-body Motion of Humanoid Robots", Proc. of ICRA, Vol. 3, pp. 3105–3110, 2002.
- [7] S. H. Collins, M. Wisse and A. Ruina, "A Three-Dimensional Passive-Dynamic Walking Robot With Two Legs and Knees", *Int. J. of Robotics Research*, pp. 607–615, 2001.
- [8] M. Wisse and J. van Frankenhuyzen, "Design and Construction of MIKE; a 2D autonomous biped based on passive dynamic walking", Proc. of 2nd Int. Sympos. on Adaptive Motion of Animals and Machines, 2003.
- [9] F. Asano, M. Yamakita, N. Kamamichi and Z. W. Luo, "A Novel Gait Generation for Biped Walking Robots Based on Mechanical Energy Constraint", Proc. of IROS, pp. 2637–2644, 2002.
- [10] K. Ono, R. Takahashi, A. Imazu and T. Shimada, "Self-Excitation Control for Biped Walking Mechanism", Proc. of IROS, pp. 1143–1148, 2000.
- [11] J. Pratt and G. Pratt, "Exploiting Natural Dynamics in the Control of a 3D Bipedal Walking Simulation", Proc. of Int. Conf. of Climbing and Walking Robots, 1999.
- [12] J. Pratt and G. Pratt, "Intuitive Control of a Planar Bipedal Walking Robot", Proc. of ICRA, pp. 2014–2021, 1998.
- [13] T. McGeer, "Passive Dynamic Walking", *Int. J. of Robotics Research*, Vol. 9, No. 2, pp. 62–82, 1990.
- [14] M. H. Raibert, *Legged Robots That Balance*, MIT Press, 1986.
- [15] R. Q. van der Linde, "Passive Bipedal Walking with Phasic Muscle Contraction", *Biological cybernetics*, Vol. 81, pp. 227–237, 1999.
- [16] B. Thuijlot, A. Goswami and B. Espiau, "Bifurcation and Chaos in a Simple Passive Bipedal Gait", Proc. of ICRA, pp. 792–798, 1997.
- [17] S. Miyakoshi, G. Cheng and Y. Kuniyoshi, "Transferring Human Biped Walking Function to a Machine - Towards the Realization of a Biped Bike-", Proc. of Int. Conf. on Climbing and Walking Robots, pp. 763–770, 2001.
- [18] G. T. Yamaguchi and F. E. Zajac, "Restoring Unassisted Natural Gait to Paraplegics Via Functional Neuromuscular Stimulation: A Computer Simulation Study", *IEEE Trans. on BME*, Vol. 37, No. 9, pp. 886–902, 1990.
- [19] R. Nakamura and H. Saitoh, *Clinical Kinematics*, ISHIYAKU Publishers, Inc., 1990 (in Japanese).
- [20] N. Yamazaki, T. Suzuki, M. Kouchi, A. Kusunoki and S. Nishizawa, *Encyclopedia of Foot*, Asakura Syoten, 1999 (in Japanese).
- [21] S. Kagami, M. Mochimaru, Y. Ehara, N. Miyata, K. Nishiwaki, H. Inoue, T. Kanade, "Measurement and Comparison of Humanoid H7 Walking with Human Being", Proc. of Humanoids, 2003.
- [22] Y. Ehara and S. Yamamoto, *Introduction to Body-Dynamics - Analysis of Gait and Gait Initiation*, ISHIYAKU Publishers, Inc., 2002 (in Japanese).